International Journal of Pharmaceutics 396 (2010) 194–203

Contents lists available at ScienceDirect

International Journal of Pharmaceutics

journal homepage: www.elsevier.com/locate/ijpharm

Pharmaceutical Nanotechnology

In vitro characterization and *in vivo* toxicity study of repaglinide loaded poly (methyl methacrylate) nanoparticles

U.M. Dhana lekshmi, G. Poovi, Narra Kishore, P. Neelakanta Reddy*

Bio Organic Chemistry Laboratory, Central Leather Research Institute (Council of Scientific and Industrial Research, Adyar, Chennai 600020, India

ARTICLE INFO

Article history:
Received 9 March 2010
Received in revised form 11 June 2010
Accepted 14 June 2010
Available online 19 June 2010

Keywords:
Repaglinide
Anti-diabetic
PMMA
Nanoparticles

ABSTRACT

With the objective to achieve prolonged drug release, especially for the treatment of diabetes mellitus, and thereby to reduce the side effects of administration of conventional dosage form, repaglinide loaded PMMA nanoparticles have been formulated. These nanoparticles have been developed by solvent evaporation method and were subjected to various studies for characterization including photon correlation spectroscopy (PCS), scanning electron microscopy (SEM) and X-ray diffraction (XRD). These studies favorably revealed that the mean particle diameter of optimized formulation was 108.3 nm and had spherical morphology with amorphous nature.

Moreover, these particles were also subjected to Fourier transform infrared spectroscopy (FTIR), differential scanning calorimetry (DSC) and thermo gravimetric analysis (TGA) for compatibility analysis between drug and polymer. The results were positive and showed that, there were no interaction between drug and polymer. The optimized formulation demonstrated favorable *in vitro* prolonged release characteristics. Experimental *in vitro* release data were substituted with available mathematical models to establish the mechanism of release of repaglinide and was found to follow zero order, diffusion and erosion mechanisms.

The *in vivo* toxicity study in albino rats showed no significant change in biochemical and pathological examinations. Hence, the designed system could possibly be advantageous in terms of prolonged release, to achieve reduced dose frequency and improve patient compliance of repaglinide.

1. Introduction

In the recent past, substantial scientific and technological advancements have been made in the research and development of rate controlled oral drug delivery systems to counter the shortcomings of physiological adversities of conventional drugs and its administration (Sunil et al., 2005). The rate controlled oral drug delivery system has given impetus to significant advancements in the pharmaceutical engineering, of novel dosage forms such as nanoparticles, which are solid colloidal polymeric carriers less than 1 μm in size (Soppimath et al., 2001; Govender et al., 1999). These nanoparticles offer great advantages right from helping to increase the stability of drugs, proteins and up to controlled drug release properties. Several attempts have been made, towards developing biodegradable polymeric nanoparticles as potential drug delivery devices. In addition to the inherent property of reduced cyto-toxicity, biodegradable polymeric nanoparticles have been found to be extremely effective in controlled and targeted drug release, and time controlled drug delivery system notwithstanding the fact that the administration is oral (Bala et al., 2004).

Diabetes mellitus is a major and growing public health problem throughout the world and is associated with increased cardiovascular mortality, so, the current exercise is focused towards anti-diabetic treatments (Nagappa, 2008).

Repaglinide (Rg), a fast and short acting meglitinide analog, is chosen as the drug candidate for polymeric nanoparticle formulation. As far as the specific properties of the repaglinide are concerned, though it possesses phenomenal anti-diabetic properties, it has only short half-life, say 1 h and has low bioavailability (50%) and poor absorption characteristics in the upper intestinal tract. Furthermore it produces hypoglycemia after oral administration (Davis and Granner, 2001). Since these drugs are intended to be taken for a long period, patient compliance is also very important and is to be looked at (Akashi et al., 1997). Headache, gastrointestinal effects, and musculoskeletal pain are also been reported by repaglinide users (Culy and Jarvis, 2001).

Nanodrug delivery system enclosed anti-diabetic drug, may improve the therapeutic efficacy of the drug and also the polymeric nanoparticles which releases the drug in a predetermined controlled manner for a prolonged duration. Thus the adverse effects, as mentioned earlier, due to conventional dose can be surmounted.

* Corresponding author. Tel.: +91 44 24911386; fax: +91 44 24911589.
E-mail address: neelakanta@clri.res.in (P.N. Reddy).

0378-5173/$ – see front matter © 2010 Elsevier B.V. All rights reserved.
doi:10.1016/j.ijpharm.2010.06.023

Many biodegradable polymers have major advantage since; they do not require removal after application. Poly (methyl methacrylate) (PMMA) is one of the most important candidates for biomedical materials because of its biocompatibility and its relatively stronger mechanical properties (Chaiwat et al., 2007).

Recently many studies are focused on safety issues of manufactured nanomaterials to minimize or eliminate their nanotoxicity before they are being widely used (Lam et al., 2004; Hoet et al., 2007; Oberdorster and Oberdorster, 2005; Wiesner et al., 2006). Compared to microparticles, the nanoparticles, due to their nanoscale and comparatively larger surface area, may interact with biological systems in a more efficient manner. They may be beneficial but sometimes might produce grave toxicity too (Piao and Zhu, 1991). Because of the nanosize and larger surface area of the nanosubstances, it is directly correlated to many essential characteristics like surface properties, chemical reactivity, physical absorption ability and permeability through cell membranes. These factors strongly dominate nanotoxicological behavior *in vivo* (Zhao et al., 2007).

The present investigation is carried out to develop and evaluate a stable nanoparticle based biodegradable delivery system using poly methyl methacrylate polymer, which would deliver repaglinide, an anti-diabetic drug, at a controlled rate for a prolonged period of time. The investigation is limited to – finding the general toxic effects of the developed nanoparticle by subacute toxicity study, assessing the histopathological effects and determining biochemical effects of polymeric nanoparticles using Wistar male albino rats.

2. Materials and methods

2.1. Materials

Repaglinide (Rg), poly (methyl methacrylate) (PMMA) and poly (vinyl alcohol) (PVA) have been procured from Sigma–Aldrich, Germany. Dichloromethane and petroleum ether were supplied by Ranbaxy Fine chemicals Ltd, New Delhi, India. The other chemicals used were of analytical grade and are manufactured in India.

2.2. Preparation of polymeric nanoparticles

Polymeric nanoparticles were prepared by solvent evaporation method using PMMA as coating material and repaglinide (Rg) as core material. Weighed quantity of drug and polymer was dissolved in suitable organic solvent, dichloromethane (organic phase). This solution was added drop by drop to the aqueous phase of PVA and homogenized using IKA T 25 Digital Ultra turrax homogenizer, at 18,000 rpm followed by magnetic stirring for 3 h. The formed Rg–PMMA nanoparticles were recovered by centrifugation (Sigma centrifuge 3K 30) at 25,000 rpm for 15 min followed by washing thrice with petroleum ether and lyophilized (Patrick et al., 1997; Govender et al., 1999).

2.3. Nanoparticle recovery

The nanoparticle (NP) recovery, which is also referred as nanoparticle yield in the literature, calculated using Eq. (1) (Govender et al., 1999).

$$\text{Nanoparticle recovery (\%)} = \frac{\text{Mass of nanoparticles recovered}}{\text{Mass of polymericnanoparticles, drug and any formulation excipent used in formulation}} \times 100 \quad (1)$$

2.4. Determination of drug incorporation efficiency

Freeze-dried nanoparticles were dissolved in dichloromethane, the common solvent for both drug and polymer (50 ml). The amount of drug in the solution was measured using Perkin-Elmer Ultraviolet spectroscopy at 243 nm (Sunil et al., 2005, 2007; Ajit et al., 2007). Drug content (%, w/w) and drug entrapment (%) were represented by Eqs. (2) and (3) respectively.

$$\text{Drug content (\%, w/w)} = \frac{\text{Mass of drug in nanoparticles}}{\text{Mass of nanoparticles recovered}} \times 100 \quad (2)$$

$$\text{Drug entrapment (\%)} = \frac{\text{Mass of drug in nanoparticles}}{\text{Mass of drug used in formulation}} \times 100 \quad (3)$$

2.5. Particle size analysis

Particle size was determined using photon correlation spectroscopy (PCS) (Malvern S4700 PCS System, Malvern, UK). For particle size analysis Rg–PMMA nanoparticles were first suspended in 100 ml of filtered water (0.2 μm filter, Ministart, Germany) and subjected to sonication for 30 s and vortex mixing for 10 s before analysis.

2.6. Scanning electron microscopy

The shape and surface morphology of the Rg–PMMA nanoparticles were examined using scanning electron microscopy (SEM) (JSM-T20, Tokyo, Japan). An appropriate sample of polymeric nanoparticles was mounted on metal stubs, using double-sided adhesive tapes. Samples were gold coated and observed for morphology, at acceleration voltage of 15 kV.

2.7. Fourier transform infrared spectroscopy

Infrared spectroscopy was conducted using Avatar 320-FT IR UK, spectrophotometer and the spectrum was recorded in the region of 4000–400 cm^{-1}.The procedure involves dispersing a sample (drug, polymer and Rg–PMMA nanoparticle preparation) in potassium bromide pellet (200–400 mg) and compressing into discs by applying a pressure of 5 ton for 5 min in a hydraulic press. The pellet was placed in the light path and the spectrum was obtained.

2.8. Thermo gravimetric analysis

Thermo gravimetric analysis was conducted to study the thermal stability of polymer, drug and Rg–PMMA nanoparticles. TGA data were obtained using a thermo gravimetric analyzer (TGA/SDTA851, Mettler, Switzerland). The sample of 5–10 mg was accurately weighed in an aluminum pan. The measurement was conducted at a heating rate of 10 °C/min under nitrogen purging.

2.9. Differential scanning calorimetry

Differential scanning calorimetry was performed using DSC-60. Approximately 2 mg of sample was accurately weighed in a DSC aluminum pan and was crimped, followed by heating under nitrogen flow (30 ml/min) at a scanning rate of 5 °C/min from 25 °C to 200 °C. Aluminum pan containing same quantity of indium was

used as reference. The heat flow as a function of temperature was measured for both the drug and drug–excipients mixture.

2.10. X-ray diffraction analysis

X-ray diffraction analysis was performed on the polymer, drug and Rg–PMMA nanoparticles. Diffraction powder patterns were obtained with a Siemens D500 diffractometer using copper potassium radiation at 35 kV.

2.11. In vitro release study

The *in vitro* release of Rg–PMMA nanoparticles was carried out thrice in stirred dissolution cells at 37.4 °C by suspending 2 ml of Rg–PMMA nanoparticulate suspension into a beaker containing 100 ml of release media (phosphate buffer saline pH 7.4). The correct *in vitro* conditions required to study the release behavior of a hydrophobic drug were maintained because repaglinide showed 2 P*k*a values at 4.16 and 6.01. Solubility of repaglinide increases 3–6 times using phosphate buffer (pH 7.4) as solvent. In water, solubility of repaglinide is 39. 82 μg/ml. In phosphate buffer (pH 7.4) the solubility of repaglinide is 140. 86 μg/ml (Chorny et al., 2002; Avinash et al., 2007; Neelam Seedhar and Mamta Kanojia, 2009). Hence, the drug release study was carried out using phosphate buffer pH 7.4. Drug release was assessed by intermittently sampling the receptor media (5 ml) at predetermined time intervals. Each time 5 ml of fresh phosphate buffer saline pH 7.4 was replaced. The amount of repaglinide released in the buffer solution was quantified by a UV spectrophotometer at 243 nm.

2.12. Evaluation of in vitro release kinetics

In order to investigate the mechanism of release, the data were analyzed with the following mathematical models: zero order kinetic (Eq. (4)), first order kinetic (Eq. (5)) and Higuchi kinetic (Eq. (6)).

$$Q_t = K_o t \tag{4}$$

$$\ln Q_t = \ln Q_0 - K_1 t \tag{5}$$

$$Q_t = K_h t^{1/2} \tag{6}$$

The following plots were made: Q_t vs. t (zero order kinetic model), $\ln(Q_0 - Q_t)$ vs. t (first order kinetic model) and Q_t vs. $t^{1/2}$ (Higuchi model), where Q_t is the percentage of drug released at time t, Q_0 is the initial amount of drug present in the formulation and K_0, K_1 and K_h are the constants of the equations. Further, to confirm the mechanism of drug release, the first 60% of drug release was fitted in Korsmeyer–Peppas model (Eq. (7))

$$\frac{M_t}{M_\alpha} = K_p t^n \tag{7}$$

where M_t/M_α are the fraction of the drug release at time t, K_p is the rate constant and "n" is the release exponent. The value of "n" is used to characterize different release mechanisms and is calculated from the slope of the plot of log of fraction of drug released (M_t/M_α) vs. log of time (Costa and Lobo, 2001)

2.13. Animals

Wistar female albino rats (180–200 g) used for this study were procured from King Institute, Guindy, Chennai, India and housed in the Institutional animal house under standard environmental conditions (23 ± 1 °C, 55 ± 5% humidity and 12 h/12 h light/dark cycle) and maintained with free access to standard diet (Hindustan Lever Ltd, Bangalore, India) and water *ad libitum*. Then animals were divided into four groups, each group containing 6 animals ($n = 6$ per groups) and housed in poly propylene cages. The protocol of animal study was approved by Institutional Animal Ethics Committee (IAEC 03/003/08).

2.14. Toxicity studies

The animals were divided into four groups and following regimen of treatment was followed

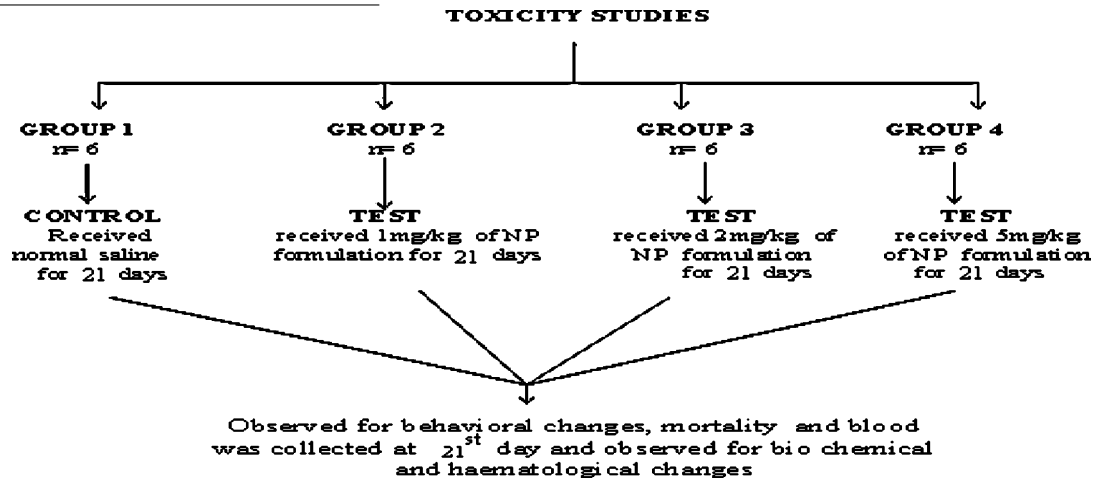

Acute toxicity was estimated by mortality and survival time, as well as by clinical picture of intoxication including behavioral reactions. Animals on study were observed for any adverse reaction, such as change in body weight, stool, condition of eye and nose, motor activity, as well as neuromuscular reactions etc. All animals examined for internal abnormalities viz. size, weight and appearance of brain, heart, lungs, liver, spleen and kidneys were assessed at necropsy (Gelperina et al., 2002). Rats were bled via the retro orbital plexus before sacrificing.

2.15. Histopathological studies

At the end of the 21st day, the animals were sacrificed and the organic tissues of heart, liver, spleen and kidneys were collected and fixed in 10% formalin then subjected to histopathological examination. The tissues of organ samples were embedded in paraffin blocks, then sliced and placed onto glass slides. After histological staining the slides were observed and photos were

Table 1
Percentage of nanoparticle recovery, drug content, entrapment and wastage for three ratios (1:2, 1:3, 1:4).

Drug–polymer preparation	Nanoparticle recovery(%)	Drug content (%, w/w)	Drug entrapment (%)	Drug wastage (%)
1:2	66.22 ± 0.55	12.41 ± 0.141	65.8 ± 0.606	34.2 ± 0.371
1:3	82.8 ± 0.266	10.99 ± 0.057	82.0 ± 0.317	18.0 ± 0.371
1:4	92.64 ± 00.059	9.75 ± 0.049	90.4 ± 0.59	09.6 ± 0.59

taken using topical microscope and histopathological examination performed.

2.16. Biochemical assays

The blood samples were centrifuged at 2000 rpm for 5 min using Sigma centrifuge. The serum was kept at −80 °C until analyzed (Gelperina et al., 2002). Levels of serum glutamate oxaloacetic transaminase (SGOT), serum alkaline phosphatase (SAP), serum gluatmic pyruvic transaminase (SGPT), serum creatinine, serum bilirubin, proteins and minerals were determined with an automatic analytical instrument Hitachi 911, Japan (Lam et al., 2004; Oberdorster and Oberdorster, 2005; Wiesner et al., 2006; Zhao et al., 2007).

3. Results and discussions

3.1. Formation of polymeric nanoparticles

The polymeric nanoparticles were prepared by solvent evaporation method with three different ratios of polymer. This method is comparatively easy to prepare than the other techniques. A suspension of polymer and drug in solvent dichloromethane forms the organic phase. This organic phase was poured into an aqueous phase containing PVA. The organic solvents used in these preparations rapidly partitioned into the external aqueous phase and the polymer precipitated around the drug particle. The subsequent evaporation of the entrapped solvent led to the formation of polymeric nanoparticles (Sunil et al., 2005).

The polymeric nanoparticles were prepared in three different ratios of PMMA polymer viz. 1:2, 1:3 and 1:4. All these ratios can be referred as repaglinide loaded poly (methyl methacrylate) preparations (Rg–PMMA). However, based on the nanoparticle recovery and drug entrapment efficiency, among the three different ratios, 1:4 ratio is selected as the best ratio than the other two. The other two ratios produced low drug entrapment which causes high drug wastage during the preparation procedure itself and showed low nanoparticle recovery, and poor yield. These have been repeatedly tried for three times, for reproducibility and for consistency. The results are elicited in Table 1.

3.2. Effect of drug content and drug entrapment

The entrapment efficiency is the function of the characteristics of polymer, drug, surfactant and cross-linking agent etc. The high entrapment efficiency is due to high affinity of drug and polymer in the same solvent – organic or aqueous solvent. The low entrapment efficiency is due to high affinity of drug and polymer in different solvents – drug in organic and polymer in aqueous solvent and or vice versa, during the nanoparticle preparation. Drug which contains carboxyl, amino and carbonyl group can form hydrogen bonding interaction with the ester group present in the polymer and drug can also form hydrophobic interaction with the aliphatic alkyl group present in the polymer chain. These non-polar groups tend to form clusters in the aqueous phase.

In Rg–PMMA nanoparticle preparation, the drug and the polymer were dissolved in the organic phase i.e., in dichloromethane and were poured into an agitated aqueous solution of poly vinyl alcohol. The drug and the polymer precipitated around dichloromethane droplets. Since the drug is hydrophophic in nature, there was no chance of diffusion of drug away from the polymer. Hence, the percentage drug entrapment of repaglinide in

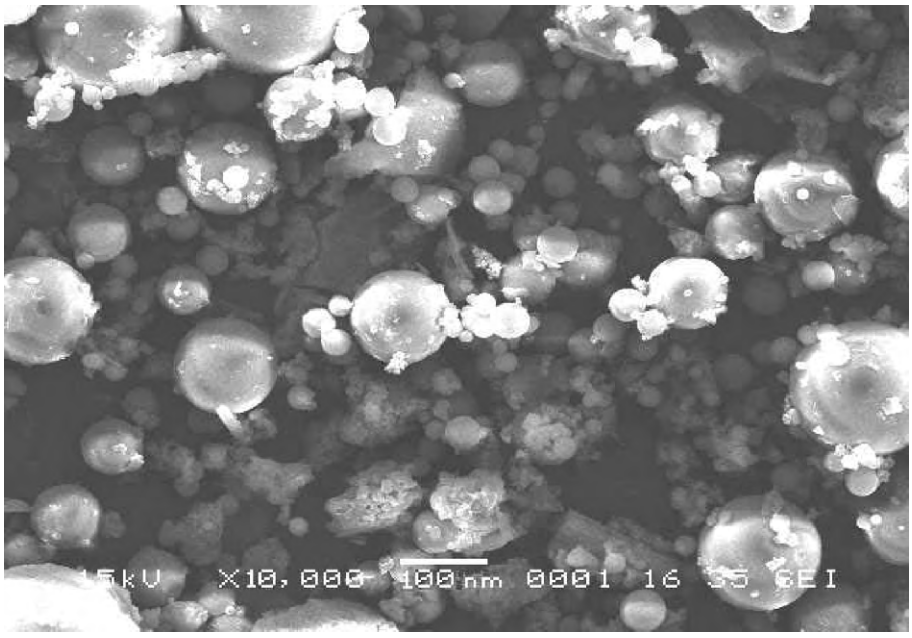

Fig. 1. Scanning electron microscopy photograph of Rg–PMMA nanoparticle.

the formulations was found to be good at all levels of drug loading. The high entrapment efficiency of repaglinide is believed to be due to its poor aqueous solubility (Sunil et al., 2005) or otherwise good solubility in the same solvent, as cited earlier. Repaglinide showed maximum absorption at 243 nm (Sunil et al., 2005, 2007; Ajit et al., 2007). The UV spectrum of pure polymer is totally transparent in the visible range and has two absorbance peaks at 298 nm and 344 nm (Majid Kazemian et al., 2007).

The drug loading and entrapment efficiency were mainly affected by the polymer and drug ratios as cited earlier. However encapsulation efficiency was proportional to the polymer ratio. This improved encapsulation efficiency was due to the greater proportion of polymer with respect to the amount of drug (Dongming et al., 2007). The ratio 1:4 was optimum, as drug wastage during nanoparticle preparation was found to be minimum. The ratios 1:2 and 1:3 delivered low yield owing to the high drug wastage and a large quantity of carrier was required to achieve sufficient amount of drug at a target site (Govender et al., 1999). Results are cited in Table 1.

The researchers (Niwa et al., 1993) attributed the decreased drug entrapment with increasing theoretical drug loadings to an enhanced drug leakage into the aqueous phase (if drug is water soluble) or into the organic phase (if drug is water insoluble) at high loadings. This would also lead to an enhanced drug loss. Compared to 1:3, 1:4 ratios, the 1:2 ratio showed high drug content and it led to an enhanced drug leakage which has been applied for our studies. The increase in drug content in the particles influence the absolute release profiles of the drug, in such a way that, it increases the induction period and the cumulative amount of drug released at any given point of time. The drug content which is closer to the surface of the nanoparticle is responsible for an increased initial burst and the drug in the core of nanoparticles is responsible for a prolonged drug release from the polymer (Avinash et al., 2007).

Although 1:2 ratio has relatively high drug content than 1:3 and 1:4 ratios, this formulation was not selected for further studies due to low drug entrapment (65%) which implies a high drug wastage during the preparation procedure, and less amount of nanoparticle recovery and increased drug release pattern. Rg–PMMA preparation of 1:4 ratio showed 9.75% (w/w) drug content, 90.4% drug entrapment and 92.64% nanoparticle recovery. High nanoparticle recovery is required for reduction of manufacturing cost. The particle size and morphology is important for quality control and biodistribution (Douglas et al., 1987) purposes which is further explained elsewhere in this paper.

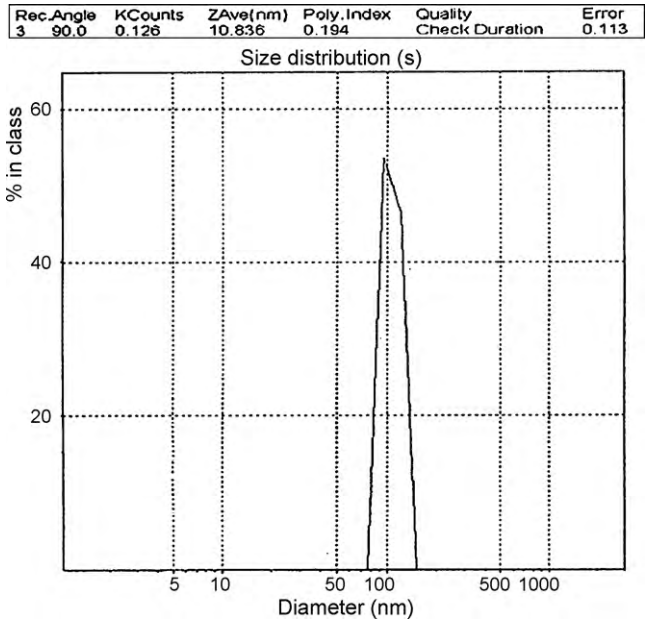

Fig. 2. PCS of Rg–PMMA nanoparticle.

3.3. Morphological characterization of polymeric nanoparticles

Fig. 1 shows that the Rg–PMMA preparation has smooth spherical shaped appearance. The surface of formulated nanoparticles depends on two factors: (1) a saturated solution of polymer, produced smooth and high yield nanoparticles. The undissolved polymer produced irregular and rod shaped particles; (2) the diffusion rate of solvent is too fast and the solvent may diffuse into the aqueous phase before stable nanoparticles are developed or formed causing the aggregation of nanoparticle preparation. In this preparation the polymer was fully saturated and the diffusion rate of solvent was minimal leading to the formation of smooth, spherical and individually homogeneously distributed particles and has no evidence of collapsed particles. Smooth surface reveals complete removal of solvent from the formulated nanoparticles and is the indication of good quality.

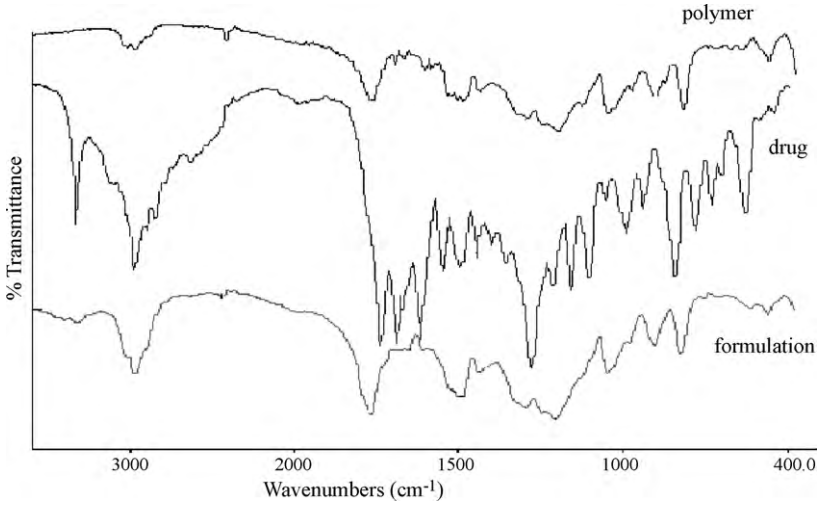

Fig. 3. FTIR of polymer, drug and Rg–PMMA nanoparticle.

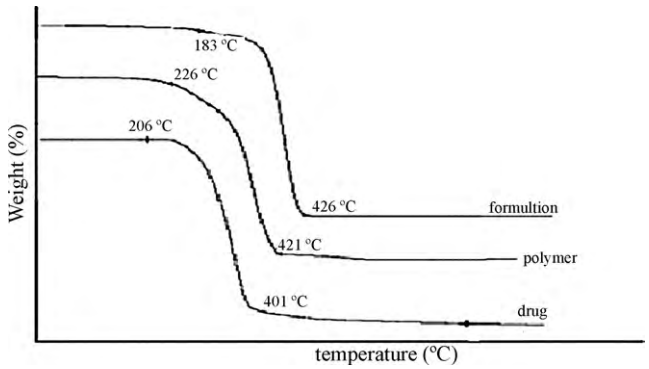

Fig. 4. TGA of Rg–PMMA nanoparticle, polymer and drug.

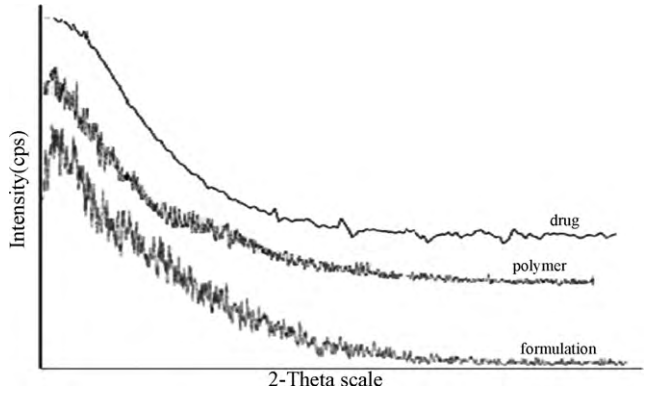

Fig. 5. XRD of Rg–PMMA nanoparticle, polymer and drug.

3.4. Particle size and poly dispersity index

Nanoparticle sizes determined by PCS are shown in Fig. 2. The particle sizes of nanoparticles were larger than those obtained by the quantitative analysis of the SEM. The explanation of this difference of PMMA nanoparticles is been given in the literature and can be employed for the charged copolymer nanoparticles as well (Finsy et al., 1992). The contrast of the electron microscope (EM) pictures allows only the visualization of the nanoparticle core, whereas the hydrodynamic radius of the particles was measured by PCS. Particle size is often used to characterize nanoparticles, because it facilitates the understanding of the dispersion and aggregation (Duane et al., 2000). Because of larger surface area and attractive force between the particles, the chance of possible aggregation is high in small sized particles. To overcome such aggregations, which were not solicited, an addition of a surfactant in the preparation was necessary. PVA appeared to be the most suitable surfactant in reducing aggregation between nanoparticles which suspends immediately after formation (Duane et al., 2000).

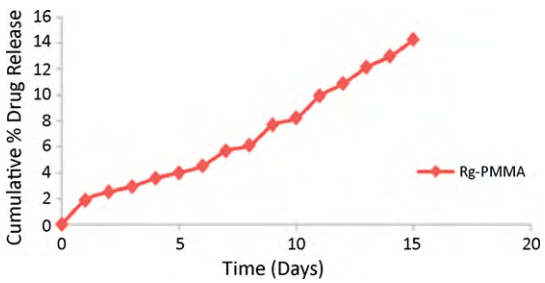

Fig. 6. *In vitro* release of repaglinide from polymeric nanoparticles of 1:4 ratio.

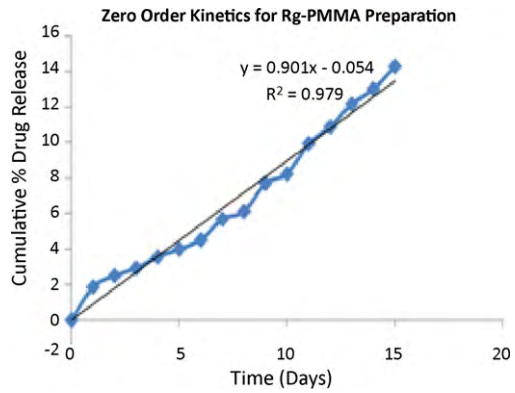

Fig. 7. Zero order kinetics data of Rg–PMMA nanoparticle preparation.

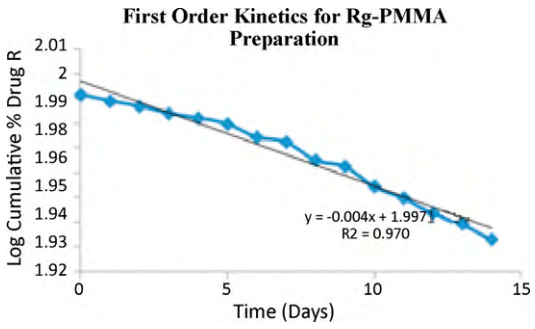

Fig. 8. First order kinetics data of Rg–PMMA nanoparticle preparation.

The particle size data showed that nanoparticles produced were of submicron size and had low poly dispersity which indicates relatively narrow particle size distribution for Rg–PMMA preparations. The mean diameter and poly dispersity index (PI) of Rg–PMMA polymeric nanoparticles was found to be 108.3 nm and 0.194 PI.

3.5. FT-infrared spectroscopy (FTIR)

FTIR spectral data were used to confirm the chemical stability of repaglinide in polymeric nanoparticle. FTIR spectra of pure repaglinide, polymer and repaglinide loaded polymeric nanoparticle are shown in Fig. 3.

The finger print characteristic vibration bands of PMMA polymer appears at 2947 cm^{-1} corresponds to the C–H stretching of the methyl group (CH_3) while the strong band at 1142 cm^{-1} are associated with saturated ester group. The band at 1727 cm^{-1} is due to (C=O stretching) ester carbonyl group and 1450 cm^{-1} (C–O bond stretching).

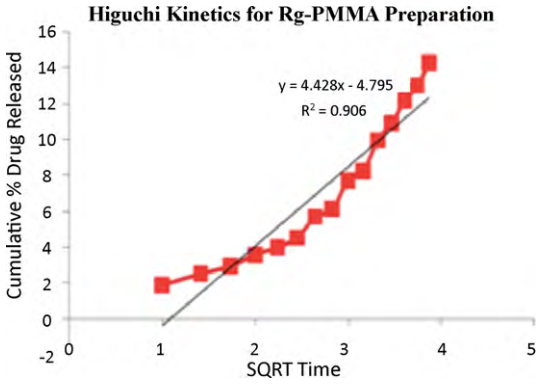

Fig. 9. Higuchi eqation data of Rg–PMMA nanoparticle preparation.

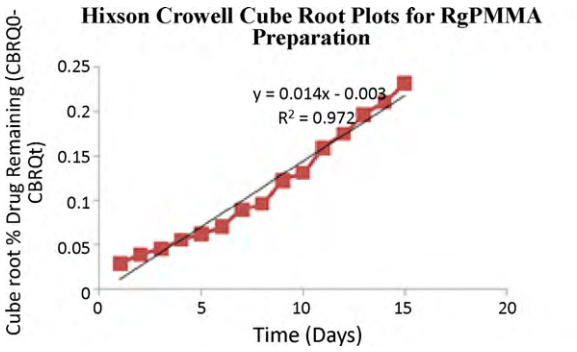

Fig. 10. Hixson–Crowell equation data of Rg–PMMA nanoparticle preparation.

FTIR of pure repaglinide showed peaks at 3320 cm^{-1} (NH stretching), 2947 cm^{-1} (CH stretching), 1728 cm^{-1} (C=O stretching). The bands at 1438 cm^{-1} and 1242 cm^{-1} are due to C–O stretching and O–H bending vibrations.

The common peaks appears both in polymer and drug polymer mixture were 1452 cm^{-1}(C–O stretching), 1247 cm^{-1}(C–O stretching of ester) and 752 cm^{-1}(aromatic CH bending). The common peaks appear both in drug and drug polymer mixture were 1385 cm^{-1} and 1149 cm^{-1}(ester C–O group), 985 cm^{-1} and 752 cm^{-1} (aromatic CH bending), respectively.

The interaction study between drug and polymer was evaluated. The characteristic band peak at 1719 cm^{-1} in repaglinide and PMMA is slightly decreased in formulation due to the intermolecular hydrogen bonding between the ester (C=O) group of polymer and carboxylic acid (–OH) group of the drug. Comparing the FTIR spectra of pure polymer, drug and formulation we confirmed that there is no significant interaction between drug and polymer and has good chemical stability.

3.6. Differential scanning calorimetry (DSC)

DSC examination was conducted for pure drug, polymer and for the drug loaded polymeric nanoparticle. Pure drug showed a sharp endotherm at 135.5 °C corresponding to its melting point/transition temperature. Polymer showed endotherm at 150 °C. Drug loaded polymeric nanoparticle showed endotherm at

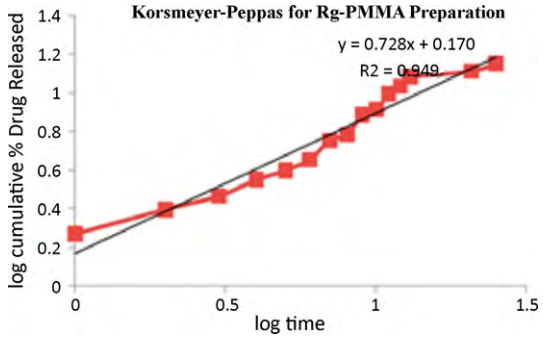

Fig. 11. Korsmeyer–Peppas eqation data of Rg–PMMA nanoparticle preparation.

Table 2
Release kinetics data of Rg–PMMA polymeric nanoparticle.

Equation	Zero order	First order	Higuchi	Korsmeyer	Hixson–Crowell
r^2	0.979	0.960	0.906	0.949	0.972

130 °C. There was no appreciable change in the melting endotherms of the formulation, compared to pure drug but slight decrease in the melting temperature had been noticed, which might be due to minor physical and morphological changes that were taking place in the drug and polymer after the formulation (Sunil et al., 2005, 2007). The difference in endotherms of polymer and formulation confirmed that there were no evidence of chemical reaction taking place between polymer and the drug (Garcia et al., 2005). The melting point of repaglinide was similar to the reported melting point of 130–131 °C (Grell et al., 1998).

3.7. Thermo gravimetric analysis (TGA)

The thermal decompositions of pure polymer, drug and formulation were studied using thermogravimetry (refer Fig. 4). Pure polymer started decomposing at above 150 °C and at 500 °C complete weight loss was observed. Repaglinide started decomposing at 206 °C and at 450 °C complete weight loss occurred. The drug loaded polymeric nanoparticle showed decomposition at 180 °C and complete weight loss at 500 °C. Since the decomposition temperatures of drug and formulation were closer, we could confirm the absence of any possible chemical interaction of drug and polymer (Ajit et al., 2007; Dongming et al., 2007).

3.8. X-ray diffraction analysis (XRD)

XRD analysis of drug, polymer and drug loaded polymeric nanoparticle were performed and are illustrated in Fig. 5. Repaglinide has shown the characteristic intense peaks at 2θ of 5.4°, 10°, 13.2°, 17.5°, 21° and 25° because of its crystallinity. However these peaks were not found in repaglinide loaded polymeric nanoparticles. There were ill-defined peaks observed in the polymer matrix. Generally, XRD peaks depend upon the crystal size. But in the present study, the drug loaded polymeric nanoparticle, the characteristic peak of repaglinide overlapped with the noise of coated polymer. From this, it is evident that XRD signals of encapsulated

Table 3
Behavioral parameters of Rg–PMMA treated Wistar albino rats.

Parameters	Results
Motor activity	Normal
Convulsions	Negative
Pilo erection	Negative
Righting reflex	Positive
Lacrimation	Normal
Salivation	Normal
Respiration	Normal
Skin colour	Normal
Body weight	No significant change
Muscle spasm	Negative

Table 4
Haematological report of Rg–PMMA treated Wistar albino rats compared with control rats.

Parameters	Control	1 mg/kg body weight	2 mg/kg body weight	5 mg/kg body weight
Haemoglobin (g %)	15.2 ± 0.108	14.633 ± 0.149	13.98 ± 0.135	14.8 ± 0.495
WBC (cells/cm)	9083 ± 30.7	8400 ± 143.7	6966 ± 392.9	7166 ± 586.89
Polymorph (%)	55 ± 1.825	57.5 ± 2.813	63.166 ± 1.01	61.33 ± 1.201
Lymphocytes (%)	31.80 ± 1.077	35.8 ± 0.83	31.5 ± 1.11	36 ± 1.46
Eoisnophills (%)	2.16 ± 0.401	2.16 ± 0.307	2 ± 0.258	3.1 ± 0.307
Monocytes (%)	1 ± 0.01	1.16 ± 0.166	1.33 ± 0.333	1.166 ± 0.307

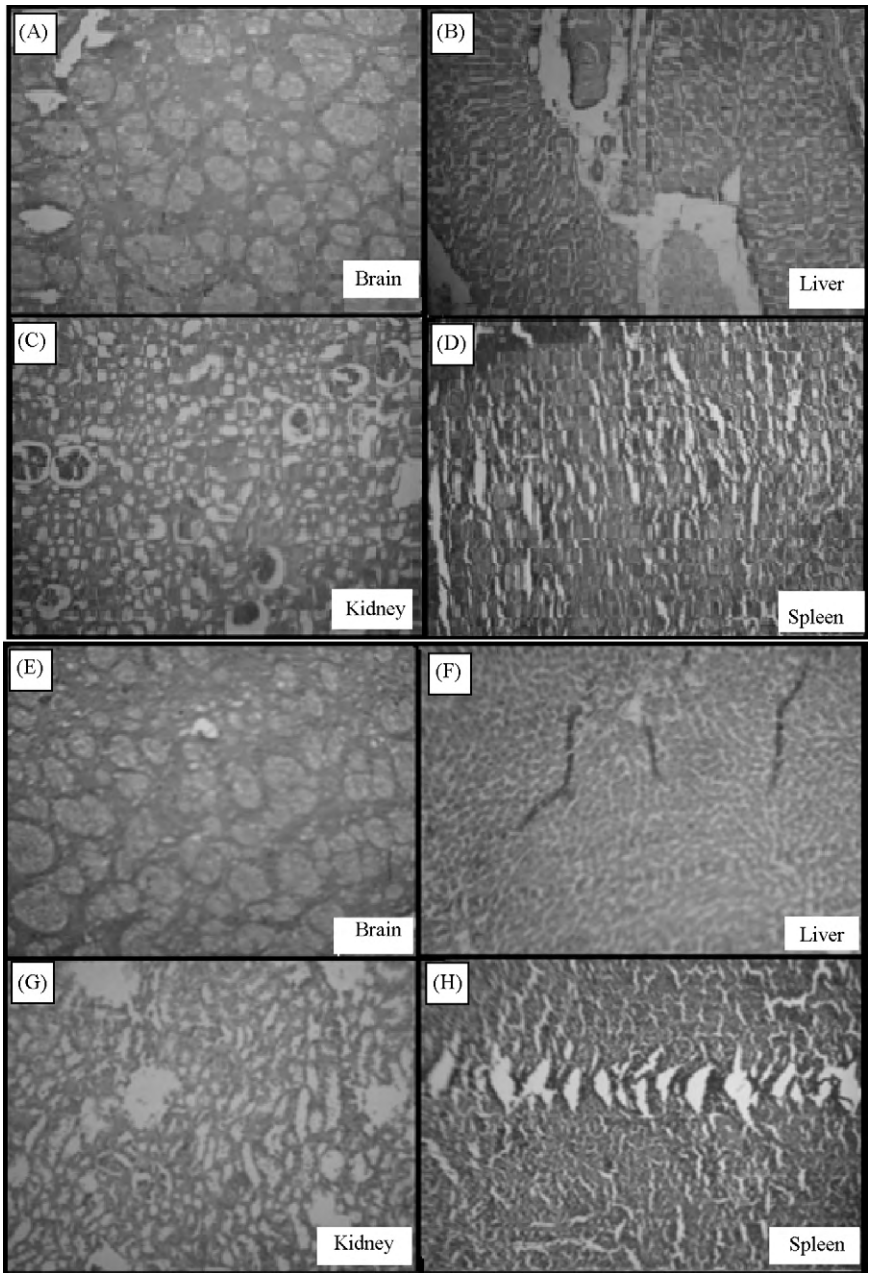

Fig. 12. Shows the histopathological slides of Wistar albino rats treated with 5 mg/kg of Rg–PMMA nanoparticle formulation compared with control. (A–D) Slide shows the brain, liver, kidney and spleen of control rats. (E–H) Slide shows the brain, liver, kidney and spleen of Rg–PMMA nanoparticle formulation rats.

drug is very difficult to detect, which shows that the drug is dispersed at a molecular level in the polymer matrix and hence no crystals are found separately in the drug loaded matrix (Liu et al., 2006; Guyot and Fawaz, 1998; Ajit et al., 2007; Dongming et al., 2007).

3.9. *In vitro* release study

The *in vitro* release of repaglinide from PMMA polymeric nanoparticles is shown in Fig. 6.

The quantity of drug released from PMMA polymeric nanoparticle preparations was as low as 14.27% for a period of 15 days. From this, it is obvious that the decreased percentage of drug release was due to the formation of a more compact wall around the drug by the polymer and it signifies that they possess a sustained drug release properties for a prolonged period of time.

3.10. *In vitro* release kinetics study

In order to determine the release model which best describes the pattern of drug release, the *in vitro* release data were substituted in zero order, first order and diffusion controlled release. The zero order rate describes, the systems, where the drug release rate is independent of its concentration. The Fig. 7 shows the cumulative amount of drug release vs. time, for zero order kinetics. The first order rate, which describes the drug release rate is dependent of its concentration. The Fig. 8 shows the cumulative percentage of drug remaining in log scale vs. time. Higuchi model describes the release of drugs from an insoluble matrix as a square root of time dependant process, based on Fickian diffusion. Fig. 9 shows the Higuchi kinetics (Sood and Pachangnula, 1998; Hamid et al., 2006). The release constant was calculated from the slope of the appropriate plots and the regression co-efficient (r^2) was determined and the results are tabulated in Table 2. In this Rg–PMMA preparation

Table 5
Biochemical report of Rg–PMMA treated Wistar albino rats compared with control rats.

Parameters	Control body weight	1 mg/kg body weight	2 mg/kg body weight	5 mg/kg body weight
Serum creatinine (μmol/l)	0.9 ± 0.1	1 ± 0.1	0.85 ± 0.12	0.92 ± 0.11
Total bilirubin (μmol/l)	0.9 ± 0.12	0.75 ± 0.11	0.80 ± 0.1	0.70 ± 0.12
SAP (IU/l)	128.5 ± 2.17	130 ± 2.63	121.1 ± 4.4	130.6 ± 3.8
Proteins (g/l)	7.51 ± 0.1740	7.3 ± 1.89	7.3 ± 0.159	7.31 ± 0.101
SGPT (IU/l)	26.16 ± 0.763	25.3 ± 0.421	25.8 ± 0.872	27.6 ± 1.66
SGOT (IU/l)	32.6 ± 0.954	29.8 ± 1.44	29.166 ± 2.3	34.1 ± 2.00
Sodium (mmol/l)	141.3 ± 0.80	140.8 ± 1.53	137 ± 0.909	135 ± 3.413
Chloride (mmol/l)	107.8 ± 2.5	106.3 ± 1.4	106 ± 1.536	105 ± 2.713
Potassium (mmol/l)	4.25 ± 0.08	4.2 ± 0.071	4.0 ± 0.21	4.0 ± 0.791
Bicarbonates (mmol/l)	26.5 ± 0.56	22.5 ± 0.562	24.83 ± 0.8	23.6 ± 0.843

the *in vitro* release kinetics was best explained by zero order equation, as the plots showed the highest linearity(r^2 = 0.979) followed by first order (r^2 = 0.970), followed by Higuchi equation (r^2 = 0.906). Hence the drug release kinetics demonstrate that the concentration was nearly independent of drug release.

The data were also plotted in accordance with the Hixson–Crowell cube root law which indicates the progressive dissolution of the matrix as a function of time and are shown in Fig. 10 (Jalehvarshosaz, 2006).

To explain the mechanism of drug release, Korsemeyer–Peppas equation has been applied (cumulative percentage drug release in log scale vs. time) and good linearity (r^2 = 0.949) has been observed. The results are plotted in graphical form in Fig. 11. The release exponent n = 0.78, which appears to be coupling of diffusion and erosion mechanism called anomalous diffusion, which indicates that the drug release is controlled by more than one process. Group of researchers also considered the corresponding "*n*" values as the indication of anamalous release mechanism (Reddy et al., 2003; Fassihi and Ritschel, 1993; Hamid et al., 2006). From these results we can conclude that the release of repaglinide from the PMMA matrix is by zero order, diffusion and erosion mechanism.

3.11. Toxicity studies

Based on the *in vitro* release characteristics and other parameters, repaglinide–PMMA preparation in the ratio of 1:4 was selected for *in vivo* toxicity studies using male albino rats. Nanosized particles can cross small intestine by persorption and further can be distributed into the blood, brain, lung, heart, kidney, spleen, liver, intestine and stomach (Hillye and Abrecht, 2001). For insoluble particles, their pathway and extent of uptake through the digestive tract are known to be size dependent (Hodges et al., 1995; Donaldson et al., 1998). The smaller sized particles show interaction with local tissues and provoke dysfunction of the organs (Piao et al., 2003). Hence toxicity study was carried out using different doses (1 mg/kg, 2 mg/kg and 5 mg/kg body weight) of nanoparticle formulation for behavioral changes, hematology parameters and biochemical parameters. These were closely examined and results are tabulated in Tables 3–5, respectively. Hematological and biochemical reports show that there are no noticeable changes in all the parameters of the nanoparticle treated group when compared with the control. The pathological examinations revealed that kidney, liver, brain and spleen were not exposed to nanotoxicity after oral administration of the nanoformulation when compared with control rats. Fig. 12 shows the histopathological slides of Wistar albino rats treated with 5 mg/kg of Rg–PMMA nanoparticle formulation compared with control. Here also, there was no observable change in the brain cells. In kidney, there was no apparent change in the glomerulus, tubules and absence of necrosis was observed. Liver showed normal hepatocytes with stained nucleolus. Spleen cells were also found to be normal when compared with control.

4. Conclusion

Repaglinide loaded poly (methyl methacrylate) nanoparticles were successfully formulated by solvent evaporation method. Different investigations on preparation, characterization, *in vitro* release and toxicity of nanoparticles were carried out and performance of the formulations was evaluated. The proposed repaglinide loaded poly (methyl methacrylate) nanoparticles illustrates an effective way, to prolong drug release. The toxicological results obtained after oral administration of nanoparticles to healthy rats were found to be satisfactory.

The developed nanoparticles are safer, and is the need of the hour for pharmaceutical industry as an alternative drug delivery system for the treatments of highly prevalent and chronic disease like type II diabetes mellitus. To optimize this drug delivery system, and for deeper understanding of different mechanisms, further studies are still required. Accordingly, the next step of this work has been planned to optimize various parameters which influence efficacy and bioavailability *in vivo*.

Acknowledgements

We are grateful to Dr. A.B. Mandal, Director, CLRI, for giving permission to publish this work. We are also thankful to Mr. V. Elango, Department of Bio Organic Chemistry Lab, for helping in animal experiments and careful maintenance of the animals during the experimental period. Author U.M. Dhanalekshmi gratefully acknowledges the support of Council of Scientific and Industrial Research, India for granting fellowships.

References

Ajit, P.R., Sanamesh, A.P., Anagha, A.B., Shivaraj, B.H., Tejraj, M.A., 2007. Preparation and evaluation of cellulose acetate butyrate and poly (ethylene oxide) blend microspheres for gastro retentive floating delivery of repaglinide. J. Appl. Polym. Sci. 105, 2764–2771.

Akashi, M., Furuya, K., Iwata, M., Onishi, H., Machida, Y., Shirotake, S., 1997. Trial for transdermal administration of sulphonylureas. Yakugaku Zassi 12, 1022–1027.

Avinash, B., Steven, J.S., Karen, I., 2007. Controlling the *in- vitro* release profiles for a system of haloperidol-loaded PLGA nanoparticles. Int. J. Pharm., 87–92.

Bala, I., Hariharan, S., Kumar, M.N., 2004. PLGA nanoparticles in drug delivery the state of art. Crit. Rev. Ther. Drug Carrier Syst. 21, 387–482.

Chaiwat, N., Qinmin, P., Garry, L.R., Suda, K., 2007. Synthesis of poly (methyl methacrylate) nanoparticles initiated by 2,20-azoisobutyronitrile via differential micro emulsion polymerization. Macromol. Rapid Commun. 28, 1029–1033.

Chorny, M., Fishbein, I., Danenberg, H.D., Golomb, G., 2002. Liphophilic drug loaded nanospheres prepared by nanoprecipitation: effect of formulation variables on size, drug recovery and release kinetics. J. Control. Release 83, 389–400.

Costa, P., Lobo, J.M.S., 2001. Modelling and comparison of dissolution profiles. Euro. J. Pharm. Sci. 13, 123–133.

Culy, C.R., Jarvis, B., 2001. Repaglinide: a review of its therapeutic use in type II diabetes mellitus. Drugs 61, 1625–1660.

Davis, S.N., Granner, D.K., 2001. Insulin oral hypoglycemic agents and the pharmacology of the endocrine pancreas. In: Hardman, J.G., Limbrid, L.E. (Eds.), Goodman and Gillman. The pharmacological basis of therapeutics. McGraw-Hill Medical Publishing Division, USA, pp. 1704–1705.

Donaldson, K., Li, X.Y., Mac, N.W., 1998. Ultrafine (nanometer) particle mediated lung injury. J. Aerosol Sci. 29, 553–560.

Dongming, P., Huang, K., Liu, Y., Lin, S., 2007. Preparation of novel polymeric microspheres for controlled release of finasteride. Int. J. Pharm. 342, 82–86.
Douglas, S.J., Davis, S.S., Illum, L., 1987. Nanoparticles in drug delivery. CRC Crit. Rev. Ther. Drug Carrier Syst. 3, 233–261.
Duane, Birnbaum, Jacqueline, Peppas, L.B., 2000. Optimization of preparation techniques for poly (lactic acid-co-glycolic acid) nanoparticles. J. Nanoparticle Res. 2, 173–181.
Fassihi, R.A., Ritschel, W.A., 1993. Multiple layer, direct compression controlled release system: invitro and invivo evaluation. J. Pharm Sci. 82, 750–754.
Finsy, R., Dejaeger, N., Sneyers, R., Gelade, E., 1992. Particle sizing by photon correlation spectroscopy. Part. Part. Syst. Char. 9, 125–137.
Garcia, M.F., Maria, J.A., Dolores, T., 2005. Design and characterization of a new drug nano carrier made from solid lipid mixtures. J. Colloid Interface Sci. 285, 590–598.
Gelperina, S.E., Khalansky, A., Smirnova, Z.S., Bobruskin, A.I., Severin, S.E., 2002. Toxicological studies of doxorubicin bound to polysorbate 80-coated poly (butyl cyanoacrylate) nanoparticles in healthy rats and rats with intracranial glioblastoma. Toxicol. Lett. 126, 131–141.
Govender, T., Stolnik, S., Martin, C.G., Illum, L., Stanley, S.D., 1999. PLGA nanoparticles prepared by nanoprecipitation: drug loading and release studies of a water soluble drug. J. Control. Release 57, 171–185.
Grell, W., Hurnaus, R., Griss, G., 1998. Repaglinide and related hypoglycemic benzoic acid derivatives. J. Med. Chem. 41, 5219–5246.
Guyot, M., Fawaz, F., 1998. Nifedipine loaded polymeric microspheres: preparation and physical characterization. Int. J. Pharm. 175, 61–74.
Hamid, A. Merchant, Harris, M. Shoaib, Jaweria Tazeen, Rabia Yousuf, 2006. Once daily formulation and in vitro evaluation of cefopodoxime using hydroxy propyl methyl cellulose – a technical note. AAPS PharmSciTech., article. 78.
Hillye, J.F., Abrecht, R.M., 2001. Gastro intestinal per sorption & tissue distribution of differently sized colloidal gold nanoparticles. J. Pharm. Sci. 90, 1927–1936.
Hodges, G.M., Carr, E.A., Hazzard, R.A., Roilly, O., Carr, K.E, 1995. A commentary on morphological and quantitative aspects of micro particle translocation across the gastro intestinal mucosa. J. Drug Targeting 3, 57–60.
Hoet, M., Chen, Z., Xing, G., Yuan, H., Chen, C., Zhao, F., Zhang, C., Zhao, Y., 2007. Ultrahigh reactivity provokes nanotoxicity: explanation of oral toxicity of nanocopper particles. Toxicol. Lett. 175, 102–110.
Jalehvarshosaz, 2006. Use of hydrophilic natural gums in formulation of sustained release matrix tablets of Tramadol hydrochloride. AAPS PharmSciTech. 7, E1–E7.
Lam, C.W., James, J.T., Mc Cluskey, R., Hunter, R.L., 2004. Pulmonary toxicity of single-wall carbon nanotubes in mice, 7 and 90 days after intratracheal instillation. Toxicol. Sci. 77, 126–134.
Liu, Y.F., Huang, K.L., Peng, D.M., Wu, H., 2006. Synthesis,characterization and hydrolysis of an aliphatic polycarbonate terpolymerisation of CO_2, propylene oxide and maleic anhydride. Polymer 47, 8453–8461.
Majid Kazemian, A., Paramanik, D., Varma, S., Gosavi, S.W., Kulkarni, S.K., 2007. Formation of gold nanoparticles in polymethylmethacrylate by UV irradiation. J. Phys. D: Appl. Phys. 40, 3771–3779.
Nagappa, A.N., 2008. Novel strategies for the therapeutic management of type II diabetes. Health Adm. 1–2, 58–68.
Neelam Seedhar, Mamta Kanojia, 2009. Co-solvent solubilisation of some poorly soluble anti diabetic drugs. Pharm. Dev. Technol. 14, 185–192.
Niwa, T., Takeuchi, H., Hino, N., Kunou, Y., 1993. Preparation of biodegradable nanospheres of water soluble and insoluble drugs with dl-lactide/glycolide copolymer by a novel spontaneous emulsification solvent diffusion method, and the drug release behavior. J. Control. Release 25, 89–98.
Oberdorster, E., Oberdorster, J., 2005. Nanotoxicology: an emerging discipline evolving from studies of ultrafine particles. Environ. Health Perspect. 113, 823–839.
Patrick, Donnell, James, Mc Ginity, 1997. Preparation of microspheres by the solvent evaporation technique. Adv. Drug Deliv. Rev. 28, 25–42.
Piao, F., Yokoyama, K., Ma, N., Yamauchi, T., 2003. Sub acute toxic effects of zinc on various tissues and organs of rats. Toxicol. Lett. 145, 28–35.
Piao, F.W., Zhu, W., 1991. Effect of lead on thyroid function and morphology in pregnant rats. C. J. Ind. Hyg. Occp. Dis. 9, 210–215.
Reddy, K.R., Mutalik, S., Reddy, S., 2003. Once daily sustained release matrix tablets of nicorandil:formulation and invitro evaluation. AAPS PharmSciTech. 4, 61.
Sood, A., Pachangnula, R., 1998. Drug release evaluation of dilitizem CR prepartions. Int. J. Pharm. 175, 95–107.
Soppimath, K.S., Kulkarni, A.R., Aminabhavi, T.M., 2001. Development of hollow microspheres as floating controlled–release systems for cardiovascular drugs: Preparation and release characteristics. Drug Dev. Ind. Pharm. 27, 507.
Sunil, K.J., Awasthi, A.M., Jain, N.K., Agarwal, G.P., 2005. Calcium silicate based microspheres of repaglinide for gastro retentive floating drug delivery: preparation and in vitro characterization. J. Control. Release 107, 300–309.
Sunil, K.J., Agarwal, G.P., Jain, N.K., 2007. Porous carrier based floating granular delivery system of repaglinide. Drug Dev. Ind. Pharm. 33, 381–391.
Wiesner, M.R., Lowry, G.V., Alvarez, P., Dionysiou, D., Biswas, P., 2006. Assessing the risks of manufactured nanomaterials. ES&T 40, 4336–4345.
Zhao, Y.L., Meng, H., Chen, Z., Zhao, F., Chai, Z.F., 2007. Dependence of nanotoxicity on nanoscale characteristics and strategies for reducing and eliminating nanotoxicity. In: Zhao, Y.L., Nalwa, H.S. (Eds.), Nanotoxicology. American Scientific Publishers, California, pp. 265–280.